Sub-shot-noise-limited measurements with Bose-Einstein condensates

J. A. Dunningham and K. Burnett

Clarendon Laboratory, Department of Physics, University of Oxford, Parks Road, Oxford OX1 3PU, United Kingdom
(Received 6 April 2004; published 2 September 2004)

We discuss practical schemes for using entangled Bose-Einstein condensates to detect phase shifts with a resolution better than the shot-noise limit. We begin by outlining a procedure for demonstrating how squeezed matter waves can be used to make measurements by simply lowering and raising a potential barrier between two condensates. The phase shift is read out by a scheme which involves releasing the condensates and studying the collapses and revivals of the visibility of the observed interference fringes. Finally we show how this scheme could be extended to measurements of other quantities such as gravity. All the steps of this process are attainable with current technology and so may provide a practical route for achieving enhanced resolution measurements with matter waves.

I. INTRODUCTION

An ongoing challenge in physics is to make measurements of physical quantities at the limit determined by quantum theory. Considerable effort has therefore been devoted to reducing the uncertainty in interferometric measurements to below the shot-noise limit, where the precision scales inversely with the square root of the total number of particles involved, n_{tot}. A number of theoretical schemes have shown that, by using macroscopic quantum interference (Schrödinger cat states), the measurement accuracy may be able to be improved to the Heisenberg limit, where it scales as n_{tot}^{-1} rather than $n_{tot}^{-1/2}$ [1–3]. The problem with these schemes, however, is that cat states are acutely sensitive to dissipation and the enhanced resolution that they offer is wiped out by the reduced resolution resulting from their short life spans [4].

An alternative approach to the use of cat states is to pass number correlated photons through a Mach-Zehnder interferometer, as proposed by Holland and Burnett [5]. In this case the phase information is encoded in the number variance of the final state rather than the mean number of atoms at each output port, as is the case for standard interferometry. This scheme is remarkably robust to loss and so overcomes the problems associated with the fragility of cat states. However, the improvement in phase resolution that it enables is rapidly eliminated when the effects of imperfect detectors are accounted for [6].

Recently there has been a theoretical discussion of how the effects of dissipation and finite detector efficiencies may be jointly overcome [7]. This involves making use of the superfluid–to–Mott-insulator phase transition to entangle and disentangle atomic Bose-Einstein condensates in an optical lattice. In this paper we discuss a practical way that this scheme may be implemented and present a method for experimentally measuring the output signal. We show that the phase shift may be deduced from the visibility of interference fringes observed when the condensates are released and allowed to overlap.

We shall first demonstrate the principle of the scheme by considering in detail how it can be used to measure the energy splitting between two eigenstates in a double-well potential and also the interaction strength between the atoms.

Once this is established, we shall show how the scheme can easily be modified to measure different quantities such as gravity. Importantly, all the steps of these schemes are achievable in the laboratory with current technology and so may provide a feasible route to achieving sub-shot-noise measurements with matter waves.

II. MEASUREMENT SCHEME

The sequence of steps for the measurement process is depicted schematically in Fig. 1. As our starting point, we consider two potential wells containing trapped atomic condensates. We assume that only a single level is relevant in each well and label the annihilation operators for an atom in these levels a and b. The initial state of the system, $|\psi\rangle$, is highly squeezed in the relative number of atoms in the two wells. This means that the relative number variance is much smaller than the total number of atoms in the system, n_{tot}—i.e.,

$$(\Delta n)^2 = \langle\psi|(a^\dagger a - b^\dagger b)^2|\psi\rangle - (\langle\psi|a^\dagger a - b^\dagger b|\psi\rangle)^2 \ll n_{tot}.$$
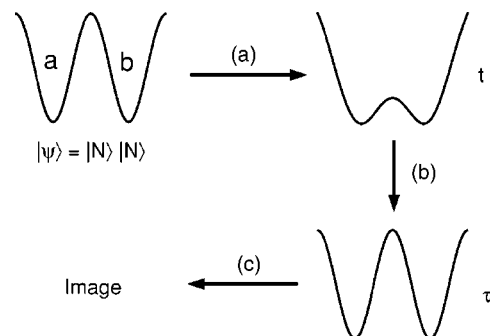(1)

FIG. 1. The measurement scheme. (a) The potential barrier between two correlated Fock state condensates is rapidly reduced and the system is allowed to evolve for time t. (b) The barrier is rapidly raised again and the system is allowed to evolve for time τ. (c) Finally the traps are turned off and an interference pattern is observed in the spatial overlap of the condensates.

70 033601-1

This initial state can be created by slowly switching on a double-well trapping potential across a condensate. The Hamiltonian that describes this system is [8]

$$H = -J(a^\dagger b + b^\dagger a) + \frac{U}{2}(a^\dagger a^2 + b^\dagger b^2), \qquad (2)$$

where J is the coupling strength between the wells, $U > 0$ is the strength of the on-site interaction energy, and we have set $\hbar \equiv 1$. As the potential barrier between the wells is increased, the coupling decreases. If this is done sufficiently slowly, the condensate adiabatically follows the ground state of the system. When the tunneling between the wells is much smaller than the interactions between atoms, the ground state has reduced fluctuations in the relative number of atoms. In extreme cases, a phase transition can occur to the Mott insulator state, for which the relative number variance vanishes, $(\Delta n)^2 = 0$, and each well contains the same number of atoms, $N = n_{\text{tot}}/2$. This phase transition has been experimentally demonstrated in condensates trapped in three-dimensional optical lattices [9].

For simplicity, we will take this highly squeezed "Mott insulating" state as the starting point for our measurement scheme:

$$|\psi\rangle = |N\rangle_a |N\rangle_b. \qquad (3)$$

In this regime, we take the coupling and interaction coefficients to have the values $J = J_1$ and $U = U_1$. We can see from Eq. (2) that this is the ground state of the system for repulsive interactions ($U_1 > 0$), since there is initially a high potential barrier separating the two wells, $J_1 \ll U_1 N$, which means we can neglect the coupling term.

The first step of our process is to rapidly reduce the barrier height [see Fig. 1(a)] so that the coupling and interaction coefficients acquire the new values J_2 and U_2, respectively. We want to do this quickly with respect to the rate of tunneling between the wells, but adiabatically with respect to the energy level spacings within the traps. The latter condition ensures that our two-mode approximation remains valid. This separation of time scales has already been experimentally demonstrated [10]. We should note that the barrier is never reduced so far that the two condensates are combined into one. This would invalidate the two-mode approximation as discussed by Javanainen and Ivanov [11].

Once the barrier has been reduced, the coupling term in Eq. (2) dominates over the interaction term, $J_2 \gg U_2 N$. It is convenient to rewrite state (3) in terms of the eigenstates of the system. These are associated with the following superpositions of the original annihilation operators:

$$\alpha = (a + b)/\sqrt{2}, \qquad (4)$$

$$\beta = (a - b)/\sqrt{2}. \qquad (5)$$

In this basis, the state has the form

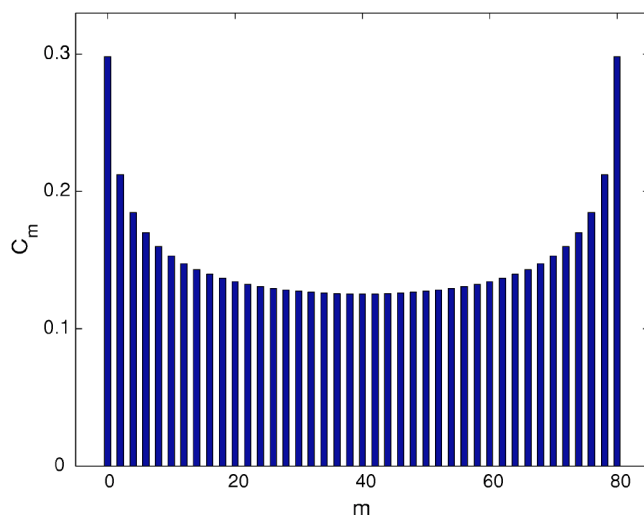$$|\psi\rangle = \sum_{m=0}^{N} (-1)^m C_m |2m\rangle_\alpha |2(N-m)\rangle_\beta, \qquad (6)$$

where

FIG. 2. Plot of the coefficients C_m given by (7) for $N = 40$.

$$C_m = \frac{\sqrt{(2m)! \, (2(N-m))!}}{2^N m! \, (N-m)!}. \qquad (7)$$

A plot of these coefficients is shown in Fig. 2 for $N = 40$. We see that the state is a superposition of different numbers of atoms in the symmetric and antisymmetric modes (4) and (5). It has the same form as the ouput from a 50:50 beam splitter with number correlated inputs [5] and is important because the width of the number distribution, Δn, is of order N. By the uncertainty relation $\Delta n \Delta \phi \sim 1$, this means that the relative phase is Heisenberg limited, $\Delta \phi \sim 1/N$.

Decoherence effects are crucial for any scheme that seeks to exploit quantum superpositions to surpass what can be achieved by classical means. Losses tend to destroy superpositions and drive the system towards classical mixtures. The state (6) will be susceptible to decoherence due to single-particle losses or quasiparticle effects when the barrier is lowered [12]. However, in previous work we showed that states of the form of Eq. (6) retain their enhanced relative phase resolution even in the presence of substantial losses [7]. We believe that this robustness feature is one of the main advantages of this scheme.

The next step is to impose a linearly varying phase across the number distribution (6). This phase is the quantity that we wish to measure and, in an interferometer, encodes the path length difference of the arms. By modifying the scheme at this point, we can vary the quantity that we measure and we will consider the measurement of different quantities later in this paper. For now we will consider the most convenient case: the two modes α and β have different energies, so, by simply holding the system for some time t and allowing the state to evolve, the modes acquire different phases. This scheme corresponds to a measurement of the energy splitting between the symmetric and antisymmetric eigenstates, $\Delta E = 2J_2$. After some hold time, t, the state is

$$|\psi\rangle = \sum_{m=0}^{N} (-1)^m e^{-i4mJ_2 t} C_m |2m\rangle_\alpha |2(N-m)\rangle_\beta, \qquad (8)$$

where we have ignored the irrelevant overall phase.

The next step of the procedure is to rapidly raise the barrier between the wells again [see Fig. 1(b)]. It is now convenient to convert the state back to the original eigenbasis of the number of atoms in trap a and in trap b. After some algebra, it can be rewritten as

$$|\psi\rangle = \frac{1}{2^N N!} \sum_{k=0}^{2N} (-1)^k D_k |k\rangle_a |2N-k\rangle_b, \qquad (9)$$

where

$$D_k = \sum_{p=\max\{0,k-N\}}^{k/2} \binom{N}{N-k+2p}\binom{N-k+2p}{p}$$
$$\times \sqrt{k!\,(2N-k)!}\,(i\sin\phi)^{N-k+2p}(2\cos\phi)^{k-2p} \quad (10)$$

and $\phi = 2J_2 t$.

For the case $\phi = 0$, we require $N-k+2p=0$ in Eq. (10) for nonvanishing values of D_k. This means that the state reduces to $|\psi\rangle = |N\rangle_a |N\rangle_b$ as we would expect, since the state has not had time to evolve at $t=0$. For the case $\phi = \pi/2$, we require $k-2p=0$ in Eq. (10). This means that, ignoring any global phase, the state reduces to

$$|\psi\rangle = \sum_{m=0}^{N} C_m |2m\rangle_a |2(N-m)\rangle_b, \qquad (11)$$

which is equivalent to the state obtained by passing Eq. (3) through a 50:50 beam splitter [5]. The broad number distribution shown in Fig. 2 is consistent with the interpretation that when two independent condensates are connected, a macroscopic superposition of different Josephson currents flow between them [12]. It turns out that for any value of ϕ, the number statistics of state (9) are precisely those obtained by passing Eq. (3) through a Mach-Zehnder interferometer with a phase difference of ϕ between the arms.

This seems to be a very convenient way of implementing the condensate interferometer scheme outlined in previous work [7]. By simply lowering and raising the barrier between the trapped condensates we can achieve interferometry with number correlated condensates. This will form the basis of our measurement schemes.

III. READ-OUT SCHEME

We would now like to consider the principal features of the output from the interferometer (9) and, in particular, study how the phase shift ϕ is encoded on it. In Fig. 3, we have plotted the variance in the number difference of atoms between the wells, $(\Delta n)^2$, as a function of ϕ for two different values of N. The crosses are the variances calculated from Eq. (9), and the solid line is a plot of

$$(\Delta n)^2 = \frac{1}{2} N^2 \sin^2 \phi, \qquad (12)$$

which fits the crosses extremely well. For small values of ϕ, the relative number variance is given by $(\Delta n)^2 \approx (N\phi)^2/2$, which means that by measuring $(\Delta n)^2$ we obtain a value for $N\phi$ and so may be able to measure phase shifts with a sensitivity that scales as $1/N$.
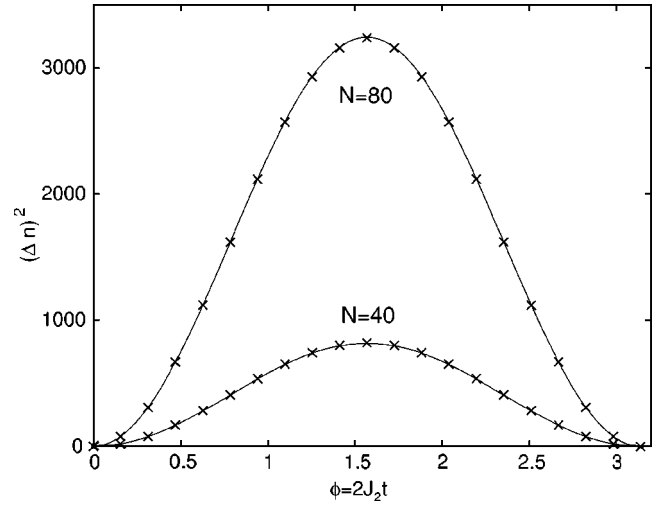

FIG. 3. The crossed curves show the number variance of state (9) as a function of ϕ for $N=40$ and $N=80$. The solid lines are given by Eq. (12).

The problem with such a scheme, however, is the measurement process itself. Kim *et al.* showed that if we were to try and measure this variance directly by number counting, we would need detectors with efficiencies better than $(1-1/N)$ in order to see any enhancement in the resolution beyond the classical limit [6]. However, in order to exploit the favorable number scaling of the phase resolution that this scheme has, we would like N to be large, which means that we would require atom detectors with almost perfect efficiencies. This makes this approach unfeasible.

In this paper, we demonstrate a technique that overcomes this crucial problem and allows the phase information to be extracted from the variances without a prohibitive dependence on the detector efficiencies. Our approach involves making use of the collapses and revivals in the relative phase between the two traps. Collapses in the order parameter have been proposed as a means of determining the state of optical [13] and atomic [14] samples and have been observed in a system of condensates trapped in an optical lattice [10]. The collapse time depends directly on the number variance of the state (12) and so may provide a means of reading out the relative phase ϕ.

Once the barrier has been raised again [Fig. 1(b)], the coupling rate between the wells is much smaller than the on-site interaction strength, $J_1 \ll U_1 N$. The system now evolves purely due to the nonlinear term. After some time τ, the state is

$$|\psi\rangle = \frac{1}{2^N N!} \sum_{k=0}^{2N} e^{i 2k(2N-k)U_1 \tau}(-1)^k D_k |k\rangle_a |2N-k\rangle_b. \quad (13)$$

The phase of each term in the superposition evolves at a different rate. Owing to the discrete nature of the superposition, at times that are multiples of $\tau = \pi/U_1$ (so-called revival times), all the phases return to the values they had at $\tau=0$. These revival times are independent of the coefficients D_k.

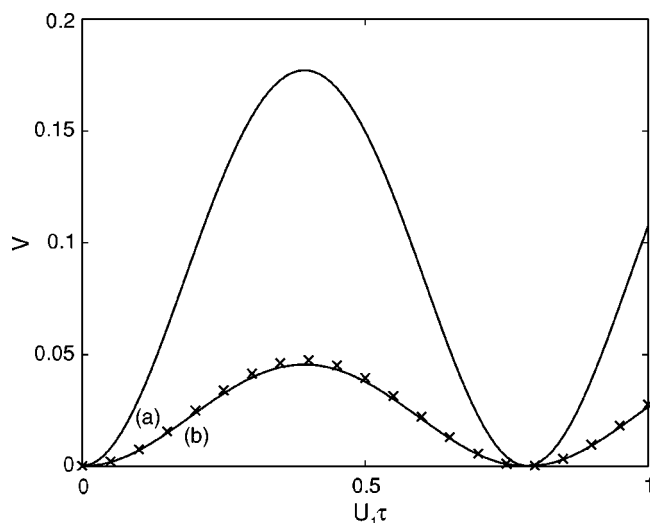The final step of our procedure [see Fig. 1(c)] is to make measurements on this state (13) and see what information we

FIG. 4. Fringe visibility as a function of $U\tau$ for (a) $N=20$ and $\phi=0.03$, (b) $N=20$ and $\phi=0.015$, and (crossed curve) $N=40$ and $\phi=0.0075$.

FIG. 5. Plot of the visibility V of the interference fringes as a function of $N\phi$ for $U_1\tau=\pi/8$.

can obtain about ϕ. The most straightforward measurement is to switch off the trapping potential of the condensates and, after some expansion time, look for interference fringes in the detected atoms [10]. On a single run, it is well known that interference fringes will be observed even if there is no initial relative phase information between the condensates [15]. The measurement process itself builds up a relative phase. On the ensemble average, however, the fringes will wash out if there is no initial phase information, but will persist if there is an initial relative phase. The visibility of the fringes therefore gives us information about the collapse time of the relative phase and hence of $(\Delta n)^2$. We would, therefore, like to calculate the visibility from Eq. (13).

We can estimate the fringe pattern on the ensemble average from the probability distribution of the relative phase between the two sites, $P(\theta)$. This distribution is given by

$$P(\theta) = |\langle\theta|\psi\rangle|^2, \tag{14}$$

where $|\theta\rangle$ is the Pegg-Barnett two-mode phase state differing by angle θ [16],

$$|\theta\rangle = \sum_{p,q} e^{ip\xi}e^{iq(\xi+\theta)}|p\rangle|q\rangle, \tag{15}$$

and ξ can take any value. For a given relative phase, θ, the fringe pattern has the form $\cos^2(x-\theta)$, where x is a spatial coordinate with arbitrary coordinates in the detection plane. The total fringe pattern for a state with a relative phase distribution $P(\theta)$ is, then,

$$F(x) \propto \int_0^{2\pi} P(\theta)\cos^2(x-\theta)d\theta, \tag{16}$$
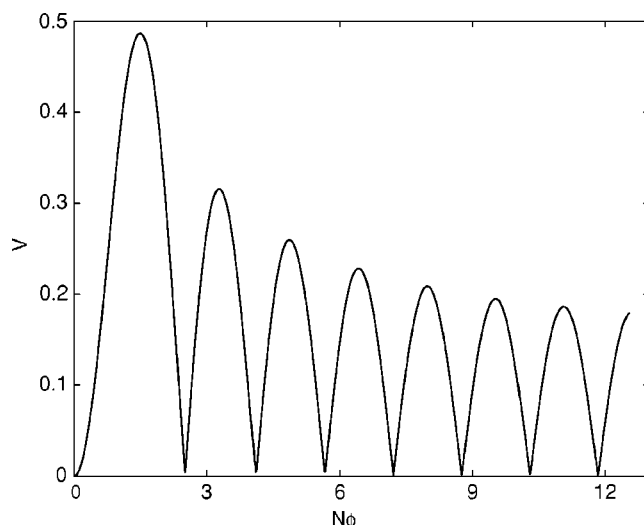
and the visibility V is given by

$$V = \frac{\max(F) - \min(F)}{\max(F) + \min(F)}. \tag{17}$$

We are now in a position to interpret the visibility in terms of the signal, ϕ.

IV. RESULTS

In Fig. 4 we have plotted how the visibility changes as a function of $U_1\tau$. We see that it oscillates, starting off at zero for $U_1\tau=0$ and building up to a maximum for $U_1\tau=\pi/8$, before decreasing again. This is in contrast to other discussions of collapses and revivals in which the order parameter initially has some finite value which decreases (collapses) as the hold time τ is increased [10,13,14].

The solid line (a) in Fig. 4 is the visibility for $N=20$ and $\phi=0.03$ and the solid line (b) is for $N=20$ and $\phi=0.015$. We see that the visibility is very sensitive to changes in ϕ. For comparison, we have also plotted as a crossed curve the result for $N=40$ and $\phi=0.0075$. This has the same value of the product $N\phi=0.3$ as the solid curve (b) and agrees with it well. Changing N and ϕ over a wide range of values reveals that the visibility curve is a function of the product $N\phi$—i.e., $V=f(N\phi)$.

We would now like to find this functional dependence. A plot of V over a range of values of $N\phi$ is shown in Fig. 5 for $U_1\tau=\pi/8$ and we see that it oscillates. In particular, there is a sequence of "lobes" over which V varies from zero to some local maximum and back to zero. These lobes have a width $\Delta(N\phi) \approx 1$, which means that by varying ϕ by of order $1/N$, the interference fringes appear and disappear on the ensemble average. This is a very clear signal which should be able to be observed experimentally and means that we should be able to distinguish phases which differ by $1/N$. In other words, this scheme has Heisenberg-limited phase resolution. This is an interesting result and can be regarded as a simple demonstration that enhanced resolution measurements can be made with squeezed atoms by a straightforward sequence of experimentally feasible steps.
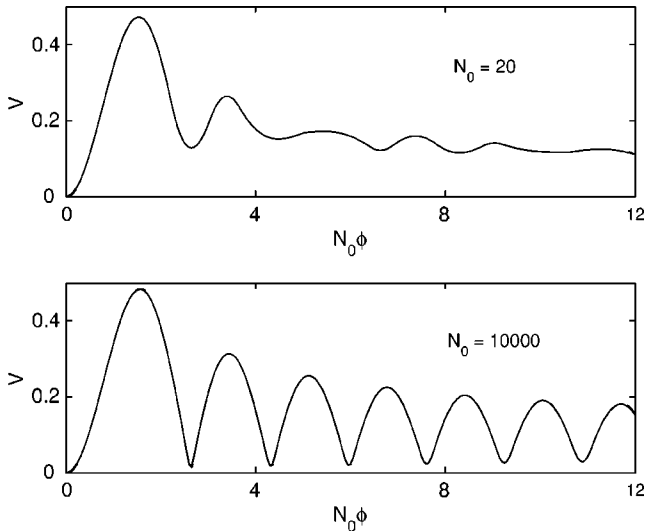
FIG. 6. Ensemble average of the visibility as a function of $N_0\phi$, where N_0 is the mean number of atoms per site.

V. NUMBER FLUCTUATIONS

The results shown in Figs. 4 and 5 would be obtained experimentally by repeating the measurement process many times and taking the ensemble average of the interference patterns. So far, our results are for the case that the total number of atoms in each run is identical. In reality, it will fluctuate between runs. In this section, we shall consider the effect that this has on our results and, in particular, see whether it swamps the Heisenberg-limited sensitivity of our scheme.

If the mean number of atoms per site is N_0 on an ensemble of runs, it seems reasonable to assume that the total number of atoms will fluctuate by of order $\sqrt{N_0}$ between runs. In Fig. 6 we have plotted the ensemble-averaged visibility of the interference fringes, V, as a function of N_0, when we allow $\sqrt{N_0}$ fluctuations on the number of atoms in each run. We should note that these fluctuations are on the total number of atoms in the system and not on the number difference between the wells. The number squeezing procedure outlined in Sec. II ensures that the number of atoms in each well is strongly correlated.

The upper part of Fig. 6 shows the result for $N_0=20$. We see that for small values of $N_0\phi$, the visibility agrees well with Fig. 5, where number fluctuations were not included. However, for values $N_0\phi > \sim 2$, the visibility lobes rapidly wash out and it would not be possible to use this technique to make measurements in this regime.

The lower part of Fig. 6 shows the result for $N_0=10\,000$. In this case, the lobes are only slightly washed out and the visibility curve agrees well with Fig. 5 over the entire plotted range. It is not surprising that the read-out signal is clearer for large values of N_0 since the $\sqrt{N_0}$ fluctuations have a smaller fractional effect in this case. A straightforward error analysis reveals that in order to measure the phase, ϕ, with resolution $1/N_0$, we require $N_0\phi < \sim \sqrt{N_0}$—i.e., $\phi < \sim 1/\sqrt{N_0}$. So this can be thought of as a technique for refining the measurement of phases within the noise of standard interferometry.

Although the signals (as shown in Fig. 6) are degraded by the fluctuations, the features of the visibility curves still vary on the scale $\phi \sim 1/N_0$. This means that the fluctuations do not destroy the Heisenberg-limited sensitivity of the scheme, which is very promising. Furthermore, the clarity of the output signal improves as N_0 is increased. This is precisely the result we want since we would like to use large numbers of atoms in this scheme to fully exploit the favorable number scaling of the phase resolution.

Finally, the need to detect many interference patterns and average over the results may be eliminated by using a lattice with more than two sites. Multisite measurement schemes have the added advantage that number squeezed arrays of condensates have already been created in the laboratory [9,17]. This is an interesting prospect that we shall explore in future work.

This completes the scheme for using condensates to make sub-shot-noise-limited measurements. So far, however, we have considered measurements only of the rather uninteresting quantity $\phi=2J_2t$. Later in this paper, we shall show how this procedure can be thought of as calibrating the condensate beam splitter and opens the door for using our scheme to make high-precision measurements of other quantities such as gravity. Before we do this, however, it is useful to consider how our scheme can also be used to precisely determine the strength of the interactions between atoms, U_1.

VI. MEASUREMENT OF U_1

In the read-out scheme outlined in Sec. III, we made use of the collapses and revivals of the interference fringe visibility. These collapses and revivals are due to the interactions between atoms and depend on the variance of the state's number distribution. In this section, we show how they can be used to accurately determine the value of U_1.

The collapse time scales inversely with the standard deviation of the number distribution [13,14], which means we would like our initial state to have a distribution with as large a width as possible in order to optimize the resolution of the scheme. We have already seen how this can be achieved. By carrying out the scheme outlined above and ensuring that $\phi=2J_2t=\pi/2$, the state that we obtain is Eq. (11)—i.e., precisely the result of passing a number-correlated state, $|\psi\rangle = |N\rangle|N\rangle$, through a 50:50 beam splitter. This state has a broad number distribution as can be seen from the coefficients plotted in Fig. 2.

If we now allow the state to evolve due to the nonlinear interactions, after some time τ, the state becomes

$$|\psi\rangle = \sum_{m=0}^{N} e^{i8m(N-m)U_1\tau} C_m |2m\rangle_a |2(N-m)\rangle_b. \qquad (18)$$

Following the same procedure as outlined above, we can calculate the fringe pattern and hence visibility of this state as a function of $U_1\tau$. The results of this are shown in Fig. 7 for $N=10$ and $N=20$ and, as expected, the visibility rapidly collapses. It then undergoes a series of minor revivals before making a full revival again at $U_1\tau=\pi/8$.

Comparing the upper and lower parts of Fig. 7, we see that as N is doubled, the widths of the revival lobes are
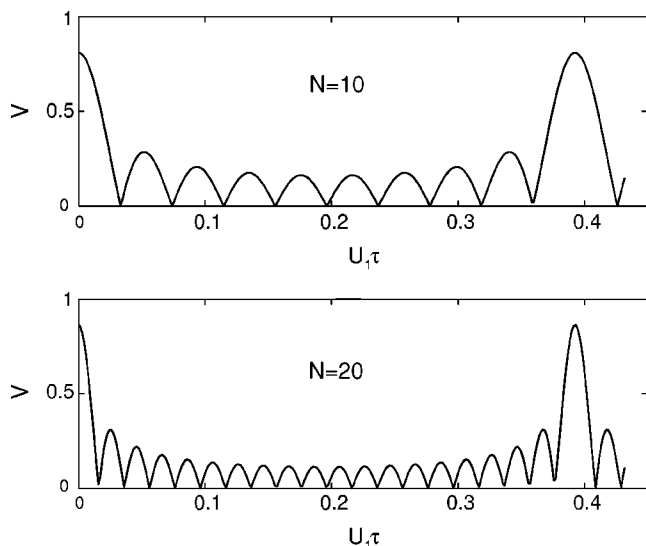
FIG. 7. Visibility of the interference fringes as a function of $U_1\tau$ for a state of the form of Eq. (11) evolving due to the nonlinear interaction between atoms for $N=10$ and $N=20$.

halved. This scaling means that we should be able to use this method to determine U_1 with $1/N$ resolution. One way would be to measure the time at which the interference visibility undergoes a full revival, $\tau=\pi/8U_1$. This time does not depend on N but, importantly, the accuracy with which we measure it (i.e., the width of the revival lobe in Fig. 7) does. This means that our method is robust to fluctuations in N between runs and so enables us to fully characterize the system by making Heisenberg-limited measurements of U_1 as well as of J_2. Armed with these results, we now finally turn our attention to how this system can be used to measure external forces such as gravity.

VII. MEASUREMENT OF GRAVITY

In order to measure gravity, we would like to create a superposition state with a large spread in the number of atoms in traps a and b. This is because, if the two traps have different positions in a gravitational field, the phases of modes a and b will evolve differently due to their different potential energies.

The initial state that we require is therefore the same one we used to measure U_1 in the previous section—i.e., the state formed by rapidly reducing the barrier between two correlated number states—allowing the state to evolve for time $t=\pi/4J_2$ and then rapidly raising the barrier again. In the first part of this paper, we showed how we could measure J_2 with Heisenberg-limited accuracy. With this knowledge, we can control $\phi=2J_2t=\pi/2$ very precisely. This can be thought of as calibrating our beam splitter with Heisenberg-limited accuracy. Our initial state is, therefore, very well described by Eq. (11).

We should note at this point that we introduce the effects of gravity only for the period of evolution between the two beam splitter operations; i.e., we do not include its effects during the state preparation and read-out stages. This could be achieved by preparing and reading out the state while the

condensates are aligned perpendicular to the gravitational field and rotating the system parallel to gravity for the phase imprinting stage. Although this may not be the most desirable configuration for practical purposes, it greatly simplifies the analysis presented here. A fuller analysis of practical issues will be presented in later work.

As before, the next step of the scheme is to simply allow the two modes to evolve and acquire different phases. In this case a and b will be subject to different gravitational fields with an energy difference $\Delta E = Mgd$, where M is the mass of an atom, g is the acceleration due to gravity, and d is the distance between the traps parallel to the gravitational field. After some hold time t, the state becomes [18]

$$|\psi\rangle = \sum_{m=0}^{N} \Omega e^{-i2m\Delta Et} C_m |2m\rangle_a |2(N-m)\rangle_b, \qquad (19)$$

where

$$\Omega = e^{i8m(N-m)U_1t} \qquad (20)$$

is the phase factor due to the nonlinear interaction evolution. Since we wish to measure ΔE, we would like to be able to ignore this complicating nonlinear phase factor (20). We can set $\Omega=1$ in the regime

$$\Delta E \gg 4NU_1, \qquad (21)$$

i.e., when the signal is much larger than the nonlinear effect. This is a somewhat restricting constraint since it sets an upper limit on N, which we would like to be large in order to improve the resolution of our schemes.

However, a much less restrictive condition can be found by noting that at revival times the nonlinear factor can be ignored. We can see from Eq. (20) that when $U_1t=p\pi/4$, where p is an integer, then Ω is unity. Now, suppose we know U_1t to within some fractional error $\delta\ll1$; then at what we think is a revival time, we have $U_1t=p\pi(1\pm\delta)/4$. Substituting this into Eq. (20) we get, $\Omega=\exp[ip2\pi m(N-m)\delta]$, since the part not proportional to δ corresponds exactly to a revival and so vanishes. If we compare Ω with the linear phase factor due to the signal in Eq. (19) at the same time, we see that we can ignore Ω if

$$\Delta E \gg 4NU_1\delta. \qquad (22)$$

This is a much less stringent constraint on N than Eq. (21). In fact, if δ scales as $1/N$, then we could arrange for it to hold for all N.

In Sec. VI, we showed how we could measure U_1t with a precision that scales as $\delta\sim1/N$. This tells us, then, how we can ignore the nonlinear phase shifts relative to the linear phase shifts of the signal, ΔE, and set $\Omega=1$ in Eq. (19). We simply ensure that the hold time t of Eq. (19) is some integer multiple of $t=\pi/4U_1$, where U_1 is precisely calibrated as outlined in the previous section.

We can now proceed with our measurement scheme. Taking state (19) with $\Omega=1$, we then repeat the calibrated 50:50 beam splitter operation to complete the interferometer; this leaves us with

$$|\psi\rangle = \frac{1}{2^N N!} \sum_{k=0}^{2N} (-i)^k D_k |k\rangle_a |2N-k\rangle_b, \qquad (23)$$

where D_k has exactly the same form as Eq. (10) with $\phi = \Delta E t = M g d t$.

This means that the output state is the same as that given by the scheme above [i.e., Eqs. (9) and (10)] apart from the relative phase between a and b. Since the signal is encoded on the number variance of the state and not on the relative phase, the relative phase is irrelevant and we can use the same technique as outlined in Sec. III to read-out the measured quantity.

Here we see why it is crucial to have a precisely calibrated 50:50 beam splitter. Since the signal we wish to measure is encoded on the state in the same way that $\phi = 2J_2 t$ is (i.e., in the same way that any variation from a perfect 50:50 beam splitter is), the final signal we measure is a combination of these two effects. This means that the beam splitter must be calibrated to the same precision with which we wish to make our final measurement. This is one of the major advantages of this scheme: the same process can be used first to calibrate the beam splitter and then to make the measurement itself.

This technique should enable us to make Heisenberg-limited measurements of the quantity $\phi = M g d t$. A plot of the visibility of the interference fringes on an ensemble average will look like the curves in Fig. 6. The fringes will vanish and reappear for variations of the phase on the scale $\phi \sim 1/N_0$. This means that we should be able to use this method to distinguish phases which differ by this amount. In an ideal system, the measurement accuracy will depend only on the total number of atoms. In practice this will be limited by (among other things) how many atoms it is possible to put into a highly squeezed state. As a guide, experiments have achieved highly squeezed states with around 1000 atoms per condensate [17]. This suggests a measurement accuracy of around 0.1%. With further work and refinement, this may be able to be significantly improved. Since t can be known very precisely, this is equivalent to a measurement of the gravitational potential energy difference between the traps, $\Delta E = M g d$. Furthermore, this scheme is quite general and should be able be used for sub-shot-noise measurements of any quantity that induces a different phase shift on the two modes a and b.

VIII. CONCLUSIONS

The ability to achieve sub-shot-noise measurements with matter waves is of great interest both from a theoretical and a practical point of view. It may lead to applications in the precision measurement of quantities such as frequencies and forces. In this paper we have outlined a straightforward procedure for making sub-shot-noise measurements of $\phi = 2J_2 t$ and $\phi = U_1 \tau$. This scheme combines simple elements such as raising and lowering a potential barrier and observing collapses and revivals of the phase between condensates. It enables us to precisely characterize our system and can be regarded as a simple proof of the principle that squeezed matter waves enable measurements to be made with enhanced precision.

After establishing this principle, we have shown how this scheme may be used to measure other quantities such as gravity. This involves using the scheme first to calibrate the beam splitter and measure U_1 and then to make the measurement itself. A key element of any measurement scheme is a method of reading-out the signal. We have introduced a technique for this that makes use of the appearance and disappearance of interference fringes. This is a clear signal that is not destroyed by imperfect detectors and could be observed experimentally. All the steps of this scheme are attainable with current technology and so may provide a practical route to achieving enhanced resolution measurements with condensates in the laboratory.

[1] D. J. Wineland *et al.*, Phys. Rev. A **46**, R6797 (1992).

[2] D. J. Wineland *et al.*, Phys. Rev. A **50**, 67 (1994).

[3] J. J. Bollinger *et al.*, Phys. Rev. A **54**, R4649 (1996).

[4] S. F. Huelga *et al.*, Phys. Rev. Lett. **79**, 3865 (1997).

[5] M. J. Holland and K. Burnett, Phys. Rev. Lett. **71**, 1355 (1993).

[6] T. Kim *et al.*, Phys. Rev. A **60**, 708 (1999).

[7] J. A. Dunningham, K. Burnett, and Stephen M. Barnett, Phys. Rev. Lett. **89**, 150401 (2002).

[8] D. Jaksch *et al.*, Phys. Rev. Lett. **81**, 3108 (1998).

[9] M. Greiner *et al.*, Nature (London) **415**, 39 (2002).

[10] M. Greiner *et al.*, Nature (London) **419**, 51 (2002).

[11] Juha Javanainen and Misha Yu. Ivanov, Phys. Rev. A **60**, 2351 (1999).

[12] I. Zapata, F. Sols, and A. J. Leggett, Phys. Rev. A **67**, 021603(R) (2003).

[13] E. M. Wright, D. F. Walls, and J. C. Garrison, Phys. Rev. Lett. **77**, 2158 (1996).

[14] J. A. Dunningham, M. J. Collett, and D. F. Walls, Phys. Lett. A **245**, 49 (1998).

[15] J. Javanainen, and S. M. Yoo, Phys. Rev. Lett. **76**, 161 (1996).

[16] S. M. Barnett, and D. T. Pegg, Phys. Rev. A **42**, 6713 (1990).

[17] C. Orzel *et al.*, Science **291**, 2386 (2001).

[18] Strictly, gravity will modify the mode functions and so change the values of J_1 and U_1. In practice, this is not a problem since J_1 is negligible and so therefore is any correction to it. The value of U_1 in the presence of gravity could be determined with Heisenberg-limited accuracy by the method outlined in Sec. VI.